

EXTENDED MAIN SEQUENCE TURNOFFS IN INTERMEDIATE-AGE STAR CLUSTERS: STELLAR ROTATION DIMINISHES, BUT DOES NOT ELIMINATE, AGE SPREADS¹

PAUL GOUDFROOIJ², LÉO GIRARDI³ AND MATTEO CORRENTI²

² Space Telescope Science Institute, 3700 San Martin Drive, Baltimore, MD 21218, USA; goudfroo@stsci.edu, correnti@stsci.edu

³ Osservatorio Astronomico di Padova – INAF, Vicolo dell’Osservatorio 5, I-35122 Padova, Italy; leo.girardi@oapd.inaf.it

Published in *ApJ*, 846, 22 (2017)

ABSTRACT

Extended main sequence turn-off (eMSTO) regions are a common feature in color-magnitude diagrams of young and intermediate-age star clusters in the Magellanic Clouds. The nature of eMSTOs remains debated in the literature. The currently most popular scenarios are extended star formation activity and ranges of stellar rotation rates. Here we study details of differences in MSTO morphology expected from spreads in age versus spreads in rotation rates, using Monte Carlo simulations with the Geneva SYCLIST isochrone models that include the effects of stellar rotation. We confirm a recent finding of Niederhofer et al. that a distribution of stellar rotation velocities yields an MSTO extent that is proportional to the cluster age, as observed. However, we find that stellar rotation yields MSTO crosscut *widths* that are generally smaller than observed ones at a given age. We compare the simulations with high-quality *Hubble Space Telescope* data of NGC 1987 and NGC 2249, which are the two only relatively massive star clusters with an age of ~ 1 Gyr for which such data is available. We find that the distribution of stars across the eMSTOs of these clusters cannot be explained solely by a distribution of stellar rotation velocities, unless the orientations of rapidly rotating stars are heavily biased towards an equator-on configuration. Under the assumption of random viewing angles, stellar rotation can account for $\sim 60\%$ and $\sim 40\%$ of the observed FWHM widths of the eMSTOs of NGC 1987 and NGC 2249, respectively. In contrast, a combination of distributions of stellar rotation velocities *and* stellar ages fits the observed eMSTO morphologies very well.

Keywords: globular clusters: general — globular clusters: NGC 1987, NGC 2249 — Magellanic Clouds

1. INTRODUCTION

Star clusters were long thought to be formed in a single burst of star formation that produced thousands to millions of stars with the same age and chemical composition, gravitationally bound together in a common potential well. However, several studies over the last ~ 15 years have shown that this traditional view oversimplified the situation. Many globular clusters (GCs) in the Local Group are now known to harbor multiple stellar populations exhibiting different abundances of light elements (see Gratton et al. 2012, for a recent review). One of the best known signatures of such multiple stellar populations is the Na-O anticorrelation among stars within clusters, which is known to exist in the great majority of globular clusters studied to date in sufficient detail (e.g., Carretta et al. 2010). The material responsible for the light element abundance variations is generally thought to accumulate in the cluster during its early evolution through slow winds of a few possible types of relatively massive stars: asymptotic giant branch (AGB) stars with masses $4 \lesssim M/M_{\odot} \lesssim 8$ (e.g., Ventura et al. 2001), or O- or B-type stars that are either rotating rapidly (Decressin et al. 2007) or in interacting binary systems (de Mink et al. 2009).

A main problem in establishing the nature of the Na-O anticorrelation in GCs has been finding out the time-scale on which the abundance variations may have occurred, which would have a direct impact on what type(s) of stars may have been responsible. Significant renewed interest in this context was created by the discovery of ex-

tended main sequence turn-offs (hereafter eMSTOs) in massive intermediate-age (1–2 Gyr old) star clusters in the Magellanic Clouds using high-quality *Hubble Space Telescope* (*HST*) data (Mackey & Broby Nielsen 2007; Glatt et al. 2008; Milone et al. 2009; Goudfrooij et al. 2009). The typical star density distribution in such eMSTOs peaks in the bright blue half and then decreases toward the faint red end, sometimes showing a ‘hump’ resembling a bimodal distribution (Mackey et al. 2008; Milone et al. 2009; Goudfrooij et al. 2011a). Furthermore, several eMSTO clusters feature a faint extension to the red clump of He-burning giants (Girardi et al. 2009; Rubele et al. 2011, 2013).

The nature of the eMSTO phenomenon is still highly debated. One common interpretation is the presence of an age spread of up to several 10^8 yr within these clusters (see also Rubele et al. 2010, 2011, 2013; Keller et al. 2011; Girardi et al. 2013; Correnti et al. 2014; Goudfrooij et al. 2014, 2015). The main scenarios that have been suggested to provide the gas required for extended star formation activity such age spreads are (1) mergers of (young) clusters with giant molecular clouds (Bekki & Mackey 2009), (2) accretion of ambient gas by the clusters (Conroy & Spergel 2011), and (3) retention of stellar ejecta in the potential well of the young clusters (Goudfrooij et al. 2011a, 2014). In this “age spread” scenario, the shape of the star density distribution across the eMSTO mainly reflects the combined effects of the histories of star formation and cluster dissolution due to strong cluster expansion following the death of massive stars in the central regions (Goudfrooij et al. 2014, hereafter G+14). Support in favor of age spreads for eMSTOs in intermediate-age clusters was provided by G+14 in the form of a correlation between MSTO width and central escape velocity, which is a proxy

¹ Based on observations with the NASA/ESA *Hubble Space Telescope*, obtained at the Space Telescope Science Institute, which is operated by the Association of Universities for Research in Astronomy, Inc., under NASA contract NAS5-26555

for the cluster’s ability to retain and/or accrete gas during its early evolution. G+14 also reported a strong correlation between the fractional numbers of stars in the bluest region of the MSTO and those in the faint extension of the red clump, as expected from an age spread.

However, non-detections of ongoing star formation in young massive clusters in nearby galaxies (Bastian et al. 2013; Cabrera-Ziri et al. 2014, 2016) have cast doubt on the interpretation of eMSTOs as being due to age spreads (but see For & Bekki 2017). The leading alternative hypothesis on the nature of eMSTOs is that it is due to a spread of stellar rotation rates. This idea was originally put forward by Bastian & de Mink (2009) who argued that rotation lowers the luminosity and effective temperature at the stellar surface (especially when viewed equator-on), which could cause an eMSTO similar to those observed. However, more recent studies revealed a stronger (and opposite) effect of stellar rotation, namely a longer main sequence (MS) lifetime due to internal mixing (Girardi et al. 2011; Ekström et al. 2012; Georgy et al. 2013), thus mimicking a younger age (i.e., a brightening and blueing of the star at a given mass).

Recently, eMSTOs have also been detected in high-quality *HST* data of much younger clusters in the Large Magellanic Cloud (LMC) with ages of ~ 100 – 300 Myr (Milone et al. 2015, 2016, 2017; Bastian et al. 2016; Correnti et al. 2015, 2017). These observations yielded several pieces of evidence in support of the rotation hypothesis. One such piece was the discovery of broadened or split main sequences which are predicted to occur if a significant fraction of stars has rotation rates Ω in excess of $\sim 80\%$ of the critical rate (Ω_C) according to the Geneva SYCLIST isochrone models of Georgy et al. (2014), whereas it cannot easily be explained by age spreads (see D’Antona et al. 2015; Milone et al. 2016; Correnti et al. 2017). Secondly, Niederhofer et al. (2015b) used the SYCLIST models and found that the presence of a distribution of rotation rates in clusters with ages up to ~ 1 Gyr causes an eMSTO whose extent, if interpreted as an age spread, is proportional to the cluster age, which is generally consistent with observations (this finding will be further assessed in Sect. 2 below). Finally, narrow-band imaging studies of some young massive clusters in the LMC reveal that several stars in their MSTOs are strong $H\alpha$ emitters and thought to constitute equator-on Be stars that are known to be rapidly rotating at $\Omega/\Omega_C \gtrsim 0.5$ (Bastian et al. 2017; Correnti et al. 2017).

While these findings render it very likely that rotation is part of the solution of the nature of eMSTOs, there are relevant indications that other effects are at play as well. For example, the distribution of stars across the MSTO of several young massive clusters with eMSTOs are *not* consistent with a coeval population of stars encompassing a range of rotation rates. Specifically, the number of stars on the “red” side of the MSTO is significantly higher than that expected if the “blue” side of the MSTO constitutes the bulk of the rotating stars in a coeval population of stars, hinting at the presence of an age spread in addition to a range of rotation rates (Milone et al. 2015, 2016, 2017; Correnti et al. 2015, 2017). Furthermore, the relatively low-mass cluster NGC 1844 with an age of ~ 150 Myr features a broadened MS as expected in the presence of a significant range of rotation rates, but does *not* exhibit an eMSTO even in high-quality *HST* data (Milone et al. 2013), in contrast to the massive 100 Myr old cluster NGC 1850 which does feature a clear eMSTO (Bastian et al. 2016; Correnti et al. 2017).

In this paper, we present a re-analysis of the expected effects of spreads of stellar rotation rates within clusters on their eMSTO morphology as a function of age, using the SYCLIST models, and we compare these effects with observations to clarify and discuss some relevant shortcomings of the rotation scenario. In Section 2, we focus on measuring the extents of eMSTOs in simulated cluster color-magnitude diagrams (CMDs) in the same way as done in practice by observers. In Section 3, we compare SYCLIST model predictions in detail with *HST* observations of two massive 1-Gyr-old eMSTO clusters, near the upper end of the range of ages for which the SYCLIST models can be used without uncertain extrapolations of the effects of rotation to the photometric properties of stars. We discuss our results in the context of the rotation and age spread scenarios in Section 4 and we state our main conclusions in Section 5.

2. EVALUATING PSEUDO-AGE SPREADS DUE TO STELLAR ROTATION

Using the Geneva SYCLIST isochrone models, Niederhofer et al. (2015b) found that the presence of a distribution of rotation rates in clusters with ages up to ~ 1 Gyr causes an eMSTO whose extent, if interpreted as an age spread, is proportional to the cluster age. As shown in Figures 1 & 2 of Niederhofer et al. (2015b), this proportionality appears when evaluating the difference in M_V near the MSTO (hereafter $\Delta M_{V, \text{MSTO}}$) between isochrones of age t_0 with $\Omega/\Omega_C = 0.0$ and $\Omega/\Omega_C = 0.5^2$ and then finding the age t_1 for which the same value of $\Delta M_{V, \text{MSTO}}$ is found when comparing non-rotating isochrones of ages t_0 and t_1 . As such, they suggested that the age spreads found in the literature may actually be due to ranges of stellar rotation rates rather than ranges of stellar ages.

However, one potential flaw in the reasoning of Niederhofer et al. (2015b) is that observational studies of intermediate-age clusters did *not* determine (pseudo-)age spreads in terms of *vertical* extents of their MSTOs on the CMD. Instead, most such studies measured the extent of the MSTO along a direction approximately perpendicular to the isochrones in the MSTO region, which is closer to *horizontal* on the CMD (i.e., parallel with color) than to *vertical* (see, e.g., Milone et al. 2009; Goudfrooij et al. 2011b, 2014; Piatti & Bastian 2016; Correnti et al. 2014, 2015, 2017). To evaluate the degree to which this changes the results of Niederhofer et al. (2015b), we conduct Monte Carlo simulations using the SYCLIST cluster models through the website described in Georgy et al. (2014)³. The differences of our method relative to that of Niederhofer et al. constitute not only the use of a more realistic definition of pseudo-ages, but also the inclusion of orientation and population effects, and observational errors. These effects cannot be considered with a simple approach that compares two isochrones.

For these simulations, we adopt the following choices: (i) the number of stars is 10,000; (ii) a random distribution of inclination angles with respect to the line of sight; (iii) gravity darkening as described by Espinosa Lara & Rieutord (2011); (iv) limb darkening as described by Claret (2000); (v) the distribution of Ω/Ω_C as described by Huang et al. (2010, hereafter HGM10). We selected this distribution because it has the highest percentage of very rapidly rotating

² The maximum amount of brightening associated with stellar rotation in the SYCLIST models is reached at $\Omega/\Omega_C = 0.5$.

³ <http://obswww.unige.ch/Recherche/evoldb/index>.

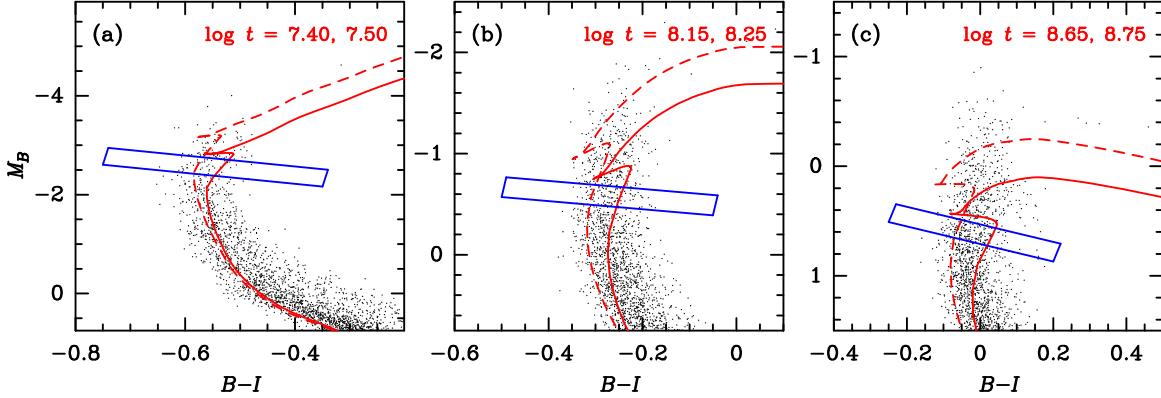


Figure 1. M_B vs. $B-I$ CMDs of SYCLIST cluster simulations of ages $\log(t/\text{yr}) = 7.50, 8.25,$ and 8.75 (in panels a, b, and c, respectively), using the distribution of rotation rates by Huang et al. (2010). Note that the axis ranges are different for each panel. SYCLIST isochrones for non-rotating stars are overplotted for ages shown in the legend of each panel (in each case, the isochrone for the first age mentioned is plotted with dashed lines). Parallelograms used to determine pseudo-age distributions are shown with blue solid lines. See discussion in Section 2.

stars (e.g., $\Omega/\Omega_C \gtrsim 0.9$) among the ones available through the SYCLIST web interface (cf. Section 3); (vi) a binary fraction of 0.3, similar to those found for young and intermediate-age clusters by many *Hubble Space Telescope* (*HST*) studies (e.g., Milone et al. 2009; Goudfrooij et al. 2011b, 2014; Milone et al. 2015, 2016; Correnti et al. 2014, 2015)⁴, and (vii) a metallicity of $Z = 0.006$. To account for photometric noise at a level that is typical for *HST* (ACS or WFC3) data of star clusters in the LMC, we use the extensive artificial star tests by Goudfrooij et al. (2011b) and G+14 to calculate the average relations between magnitude and magnitude error (σ) among their 16 intermediate-age clusters in the LMC at the core radius of the clusters in question. This is done for filters close to Johnson B (i.e., $F435W$ for ACS data and $F475W$ for WFC3 data) and Cousins I (i.e., $F814W$ for ACS and WFC3 data). Magnitude errors are added to the simulated magnitudes (assuming $m-M = 18.50$ at the distance of the LMC) by drawing random numbers from a Gaussian distribution using values of σ from the relation mentioned above. We assume that the photometric errors derived this way constitute an adequate estimate for the great majority of recent high-quality observations of star clusters in the LMC with the ACS and WFC3 cameras aboard *HST*. This includes all data shown below in Figure 2 with the possible exception of those of Niederhofer et al. (2015a) who used somewhat lower quality data from the WFPC2 camera.

To determine “pseudo-age spreads” for these SYCLIST cluster simulations in a way similar to that done for the majority of studies of eMSTO clusters using *HST* photometry, we measure the positions of stars along the long axis of a parallelogram drawn across the eMSTO in a M_B vs. $B-I$ CMD in a direction approximately perpendicular to the non-rotating isochrones and hence approximately parallel to age for non-rotating stars (for a full description of such pseudo-age distributions, see Goudfrooij et al. 2011a). The long axis of such parallelograms, which are illustrated in Figure 1 for three examples of simulated clusters with ages in the range $10^{7.5} - 10^{9.0}$ yr, are translated to pseudo-ages of non-rotating models in the following way. First we produce a grid of non-rotating SYCLIST isochrones covering the extent of the eMSTO, and then use a least-squares fit to determine the relation between age and the coordinate along the long axis of the parallelo-

gram; this relation is then used to convert the position of any simulated star –rotating or not– into a pseudo-age. Representative pseudo-age spreads of the simulated clusters are then determined by measuring the FWHM of their pseudo-age distributions.

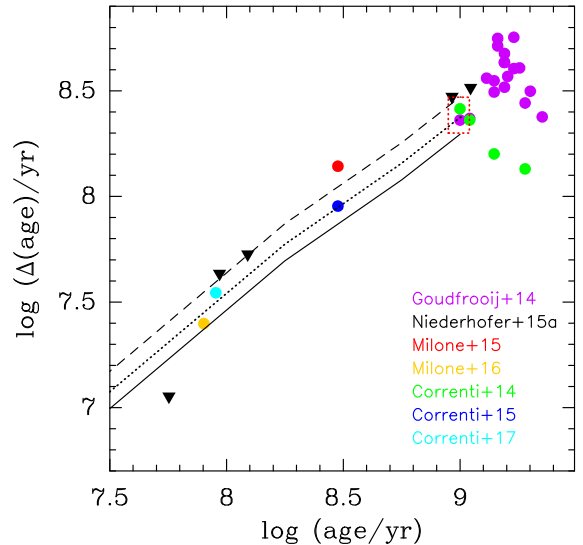


Figure 2. Predicted versus observed relations between pseudo-age spread in eMSTO clusters in the Magellanic Clouds and their age. The solid black line represents the prediction if a wide range of stellar rotation rates is interpreted as an age spread according to the SYCLIST models, based on FWHM values of pseudo-age distributions of simulated clusters as described in the text. For comparison, the dotted and dashed black lines show the same for age spreads that are larger than those indicated by the solid line by 20% and 50%, respectively. The filled symbols represent observed pseudo-age spreads of young and intermediate-age clusters. Colors indicate the respective studies as shown in the legend. The data points for NGC 1987 and NGC 2249 are surrounded by a dotted box. Note that the SYCLIST model predictions are only available for ages $\lesssim 10^9$ yr.

The results are shown as a solid black line in Figure 2, which compares these results to the FWHM pseudo-age spreads measured for real clusters in the same age range by various authors using different methods⁵ (G+14, Niederhofer et al. 2015a; Milone et al. 2015, 2016; Correnti et al. 2014, 2015, 2017). The overall picture is simi-

⁴ The results of these simulations are insensitive to the chosen binary fraction since the crosscuts through the MSTO are done in a region where the binary sequence joins that of single stars.

⁵ As such, we multiplied the standard deviation values of Niederhofer et al. (2015a) by a factor $\sqrt{8 \ln 2}$ prior to plotting.

lar to that described by [Niederhofer et al. \(2015b\)](#) in the sense that the inferred pseudo-age spreads are proportional to the actual ages of the clusters. However, the *absolute* pseudo-age spreads inferred for a given age when measured across the width of the eMSTO as mentioned above are smaller than those evaluated by [Niederhofer et al. \(2015b\)](#). The net result is that the pseudo-age spreads measured in the literature for many clusters in the age range of $10^{7.5} - 10^{9.0}$ yr are $\approx 20 - 50\%$ larger than can be accounted for by a coeval population of stars encompassing a large range of rotation rates according to the SYCLIST models. This result will be discussed further below.

3. COMPARISON WITH OBSERVATIONS OF NGC 1987 AND NGC 2249

To illustrate the impact of the analysis shown in the previous section to the nature of eMSTO's in intermediate-age clusters, we compare the SYCLIST isochrone models with high-quality *HST* photometry of NGC 1987 and NGC 2249, two eMSTO clusters in the LMC with ages of ~ 1 Gyr. These clusters were selected for this purpose for two main reasons. Firstly, their age is very close to the oldest age for which the relevant part of the MSTO still consists of stars with $\mathcal{M} \geq 1.7 M_{\odot}$ at $Z = 0.006$, so that the SYCLIST models can still be used without having to rely on extrapolations of rotational correction factors. The latter are needed at $\mathcal{M} < 1.7 M_{\odot}$, where stellar atmospheres undergo complex transitions that have a significant (but difficult to quantify) impact on stellar rotation: the transition from a convective to a radiative core and the transition from a radiative to a convective envelope. Secondly, the color spread covered by eMSTOs is larger for older ages, allowing their morphology to be studied in more detail than in younger clusters.

The *HST/ACS* photometry of NGC 1987 was described before by [Goudfrooij et al. \(2011b\)](#), (*F435W* and *F814W* filters), while the *HST/WFC3* photometry of NGC 2249 was described by [Correnti et al. \(2014\)](#), (*F438W* and *F814W* filters). The data files are available at the STScI MAST Archive ([10.17909/T9Q606](https://archive.stsci.edu/missions/hst/acs/observing/10.17909/T9Q606)). To compare the SYCLIST isochrone models with these *HST* datasets, we proceed as follows. For the SYCLIST isochrones of non-rotating stars, we first integrate the specific intensities of the ATLAS9 model atmospheres of [Castelli & Kurucz \(2003\)](#) over the projected stellar surface, and convolve the emerging model spectra with the *HST* filter transmission curves available through SYNPHOT ([Laidler et al. 2008](#)) to calculate absolute magnitudes in the *HST* passbands. For the resulting isochrones, we determine linear relations between *I* and *ACS/F814W*, *I* and *WFC3/F814W*, *B-I* and *F435W-F814W*, and *B-I* and *F438W-F814W* for stars within the intervals of $\log L$ and $\log T_{\text{eff}}$ that cover the full extent of the MSTO region in the CMD. These relations were then applied to the *B* and *I* magnitudes in the SYCLIST isochrones (for any value of Ω/Ω_C) to derive magnitudes in the *HST* passbands.

CMDs of NGC 1987 and NGC 2249 are presented in Figures 3 and 4. In order to keep the contamination of the MSTO by LMC field stars to negligible levels, we select stars in NGC 1987 within its core radius, while for NGC 2249, we select stars within its effective radius. For each cluster, we use the non-rotating Geneva isochrones for $Z = 0.006$ from [Mowlavi et al. \(2012\)](#) to find combinations of age, distance modulus ($m-M$), and reddening (A_V) to provide a good fit to the cluster's MS and the middle of its MSTO. For the same combinations of age, $m-M$, and A_V , we then overplot

the SYCLIST isochrones from [Georgy et al. \(2013\)](#) for various values of Ω/Ω_C to illustrate the effect of the ‘‘apparent rejuvenation’’ caused by a distribution of rotation rates to the extent of the MSTO⁶. After comparing this set of isochrones to the data, the age is adjusted slightly until we obtain a good fit to both the top and the left edge of the MSTO (by the isochrones with $\Omega/\Omega_C \geq 0.5$). The resulting sets of isochrones are shown in panel (a) of Figures 3 and 4.

As mentioned in the previous Section, the vertical extent of eMSTOs is well fitted by a set of single-age isochrones that represent a wide distribution of stellar rotation rates, as also emphasized by [Niederhofer et al. \(2015b\)](#). This is the case for both NGC 1987 and NGC 2249. However, it is also apparent that the eMSTO in both clusters extends to significantly redder colors than those covered by the set of isochrones representing different rotation rates. To test whether this discrepancy can be accounted for by the cumulative effects of different inclination angles of rotating stars with respect to the line of sight as well as gravity and limb darkening, we conduct Monte Carlo simulations using the SYCLIST cluster models at the ages of NGC 1987 and NGC 2249 as described in Section 2 above. Since these cluster models only involve stars with $\mathcal{M} \geq 1.7 M_{\odot}$, the number of stars in these particular simulations was chosen to be equal to the observed number of cluster stars in the MSTO and post-MS regions on the CMD, rounded to the closest hundred. Since there is no a priori knowledge of the distribution of Ω/Ω_C in these clusters, we create separate simulations for all such distributions available in the SYCLIST models, namely those of [Huang & Gies \(2006, hereafter HG06\)](#), [Huang et al. \(2010, hereafter HGM10\)](#), and a flat distribution. In addition, we create simulations for a bimodal distribution in which 2/3 of the stars rotate very rapidly ($\Omega/\Omega_C = 0.9$) while the remaining stars have negligible rotation ($\Omega/\Omega_C = 0.0$). This distribution was shown by [D'Antona et al. \(2015\)](#) to provide a good fit to the observed morphology of the split MS in the young massive LMC cluster NGC 1856 (see also [Bastian et al. 2017](#); [Correnti et al. 2017](#)). While intermediate-age clusters like NGC 1987 and NGC 2249 do not exhibit split MSes, this is likely due to their MS stars having masses $\mathcal{M} < 1.7 M_{\odot}$ which feature magnetic braking as well as less effective mixing of envelope material into the core than do stars with $\mathcal{M} > 1.7 M_{\odot}$ (see Sect. 4.1.2; [Brandt & Huang 2015](#)). As such, the absence of split MSes in these clusters does not necessarily equate to the absence of a bimodal distribution of Ω/Ω_C .

Panels (b) – (d) in Figures 3 and 4 illustrate the MSTO morphologies produced by the SYCLIST cluster models described above, for the three different Ω/Ω_C distributions. Note that the effect of random inclinations in conjunction with gravity and limb darkening can indeed have a significant impact on the resulting MSTO morphology of ~ 1 -Gyr old clusters. Specifically, the red end of the eMSTO can be populated by equator-on rapid rotators, which is especially apparent for the Ω/Ω_C distribution of HGM10. As such, the full extent of the eMSTOs of these clusters can in principle be covered by a coeval population of stars with varying rotation rates. This is consistent with the findings of [Brandt & Huang \(2015\)](#).

However, the *distribution* of stars across the eMSTO in these clusters turns out to be significantly different from

⁶ For a given age, Z , \mathcal{M}/M_{\odot} , and filter passband, the [Georgy et al. \(2013\)](#) isochrones for $\Omega/\Omega_C = 0.0$ are offset from the [Mowlavi et al. \(2012\)](#) ones by a few hundredths of a magnitude due to differences in the input physics. This offset was applied to the [Georgy et al. \(2013\)](#) isochrones here.

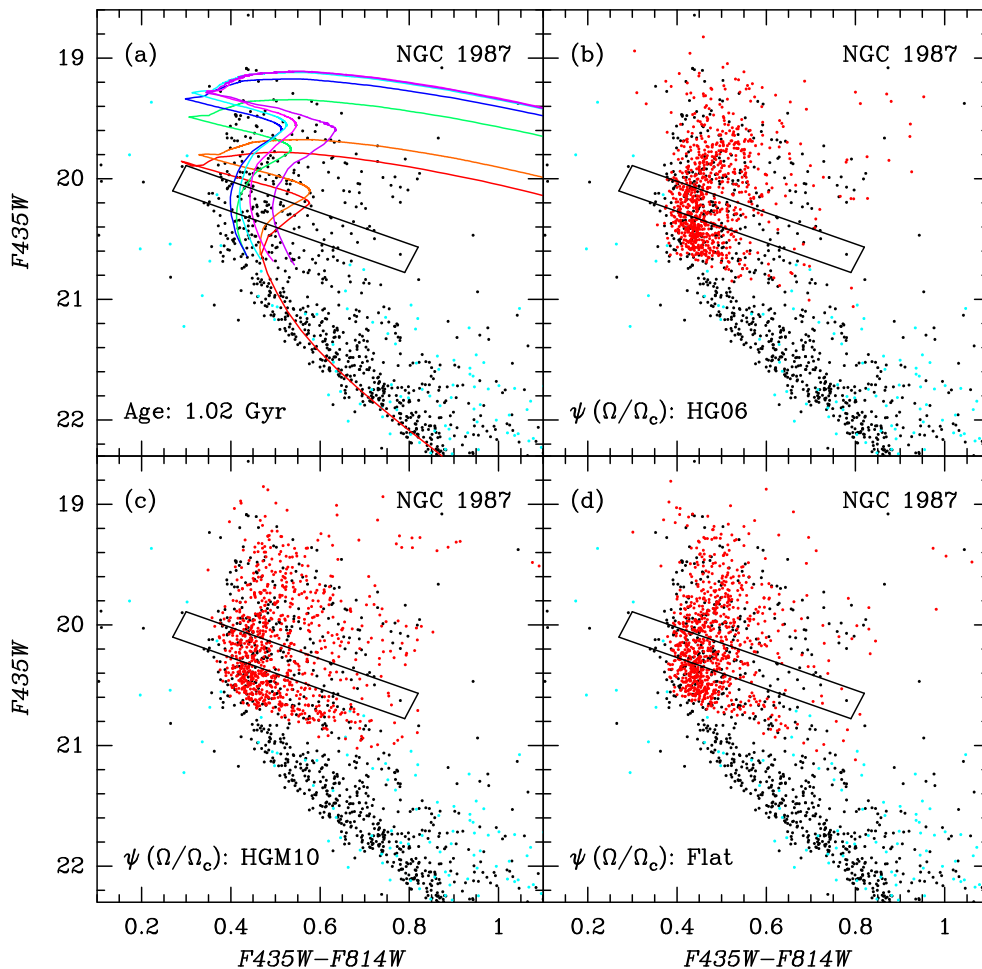


Figure 3. Upper MS and MSTO regions of CMD of NGC 1987. In all panels, the black dots represent stars within the core radius of NGC 1987 while cyan dots represent stars in a background region of the image of NGC 1987 with the same area as that shown by the black dots. The parallelogram used to derive pseudo-age distributions (see Sect. 3) is also shown in all panels. *Panel (a):* the overplotted lines represent SYCLIST isochrones for an age of 1.02 Gyr and the following values of Ω/Ω_C : 0.00 (red line), 0.10 (orange line), 0.30 (green line), 0.50 (blue line), 0.70 (cyan line), 0.80 (magenta line), and 0.90 (purple line). *Panel (b):* the red dots represent a simulated cluster using the SYCLIST models for an age of 1.02 Gyr and the Ω/Ω_C distribution of HG06. *Panel (c):* same as panel (b) but now for the Ω/Ω_C distribution of HGM10. *Panel (d):* same as panel (b) but now for a flat distribution of Ω/Ω_C .

that predicted by the SYCLIST models under the assumption of random inclination angles. To illustrate this, we derive pseudo-age distributions of the two clusters, as well as their respective SYCLIST cluster simulations⁷, in the way described in Section 2. These are shown in Figures 5 and 6 using solid lines of different colors. Note that the red (or “old”) half of the pseudo-age distributions of both clusters contain significantly more stars (relative to the peak in the blue or “young” half) than those in any of the single-age SYCLIST simulations, especially in the case of NGC 2249.

4. DISCUSSION

4.1. Constraints on The Rotation Scenario

4.1.1. Constraints from NGC 1987 and NGC 2249

Attempting to put the discrepancy between the observed pseudo-age distributions in NGC 1987 and NGC 2249 and the various single-age SYCLIST simulations in context, we first consider the relative impacts of (i) gravity and limb darkening, and (ii) the distribution of inclination angles of rotating stars with respect to the line of sight. To address point (i), we

use the same SYCLIST cluster simulations and use the values of $\log L$ and $\log T_{\text{eff}}$ that do *not* include the effects of gravity and limb darkening. To address point (ii), we only select stars in the simulations that have moderate viewing angles i of $40^\circ \leq i \leq 50^\circ$. The pseudo-age distributions of those two cases are shown for the HGM10 distribution of Ω/Ω_C in Figures 7 and 8 as dashed and dotted lines, respectively. Note that the two effects have very similar impacts on the resulting pseudo-age distribution. If we accept the magnitude of gravity and limb darkening effects as implemented in the SYCLIST models, it follows that the only way to make these models fit the observed pseudo-age distributions of NGC 1987 and NGC 2249 in an adequate manner is to require not only a distribution of Ω/Ω_C that includes a substantial fraction of very rapid rotators ($\Omega/\Omega_C \gtrsim 0.90$), but also a *distribution of viewing angles that is strongly skewed toward equator-on configurations*. This is illustrated by the magenta dot-dashed lines in Figures 7 and 8, which show the pseudo-age distributions of stars in the simulations that have viewing angles close to equator-on: $80^\circ \leq i \leq 90^\circ$. These curves provide a significantly improved fit to the observed pseudo-age distributions, especially for the case of NGC 1987. While it may seem intuitively unlikely that the viewing angles of rotating stars within a star cluster would only cover such a small range, a recent

⁷ The pseudo-age distributions of the SYCLIST simulations shown in Figures 5 and 6 constitute averages of 15 simulations each.

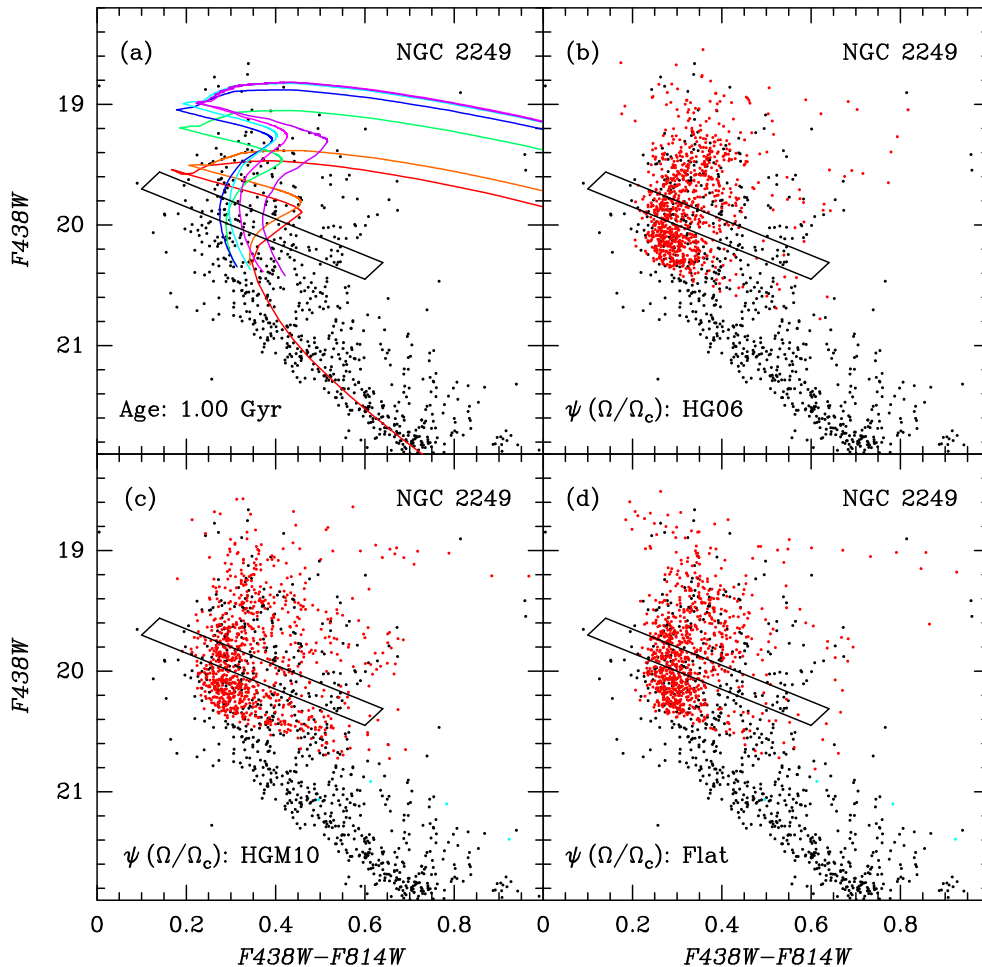


Figure 4. Same as Figure 3, but now for NGC 2249. The SYCLIST isochrones are for an age of 1.00 Gyr in this case.

asteroseismology study of two Galactic open clusters did recently find the rotation axes of $\sim 75\%$ of the observed red giant stars in each of those clusters to be closely aligned with each other (Corsaro et al. 2017), suggesting that the kinetic energy of proto-cluster molecular clouds can be dominated by rotation (rather than turbulence) which can in turn be transferred to its constituent stars during the star formation process in an efficient manner.

However, the fact that one would need the viewing angles to be close to equator-on for the rotation scenario to work for both NGC 1987 and NGC 2249 seems suspect. The probability that an intrinsically random viewing angle is $80^\circ \leq i \leq 90^\circ$ for two clusters is ~ 0.01 ; taking into account that the real distribution of Ω/Ω_C may be different from those supported in the SYCLIST models, the actual probability may be slightly higher than that but should not exceed a few per cent. Furthermore, the pseudo-age distributions of NGC 1987 and NGC 2249 are narrower than those of most other intermediate-age clusters in the Magellanic Clouds, rendering it unlikely that rotation alone (as implemented in the current SYCLIST models) can explain the eMSTO widths of all such clusters. This is discussed further in Section 4.1.2.

Comparing the observed pseudo-age distributions of NGC 1987 and NGC 2249 with the simulations that represent the bimodal distribution of Ω/Ω_C advocated by D’Antona et al. (2015; see Figures 5b and 6b), we note that the latter simulations produce star densities that are significantly lower than the observed ones at both low and high pseudo-age values

(i.e., the “top left” and “bottom right” ends of the eMSTO, respectively). As shown by panel (a) of Figures 3 and 4, stars in the top left of the eMSTO correspond mainly to stars with $0.2 \lesssim \Omega/\Omega_C \lesssim 0.8$ in the rotation scenario. As such, the lack of stars in this region in the simulation representing the D’Antona et al. (2015) distribution suggests that the distribution of Ω/Ω_C in these clusters is more uniform than purely bimodal ($\Omega/\Omega_C = 0.0$ and 0.9) in the context of the stellar rotation scenario. Conversely, the relative lack of stars in the bottom right of the eMSTO can only be explained in the rotation scenario by assuming a very high proportion of equator-on viewing angles, as discussed above.

4.1.2. Constraints from clusters with ages 1.4–2.0 Gyr

While the general correlation between MSTO extent and age among eMSTO clusters first shown by Niederhofer et al. (2015b) is quite well established among clusters with ages $\lesssim 1$ Gyr (see also Section 2), there are some features of eMSTOs among clusters in the Magellanic Clouds with somewhat older ages (~ 1.4 – 2.0 Gyr) that seem to challenge the rotation hypothesis. These are described below.

One such feature is that relative to the two 1-Gyr-old clusters studied in this paper (NGC 1987 and NGC 2249), the average width of eMSTOs increases with cluster age, peaking around an age of 1.5–1.6 Gyr, followed by a decrease (see, e.g., G14; Niederhofer et al. 2015b; Piatti & Bastian 2016)⁸.

⁸ The age where the peak average width of the eMSTOs occurs is ≈ 2.0

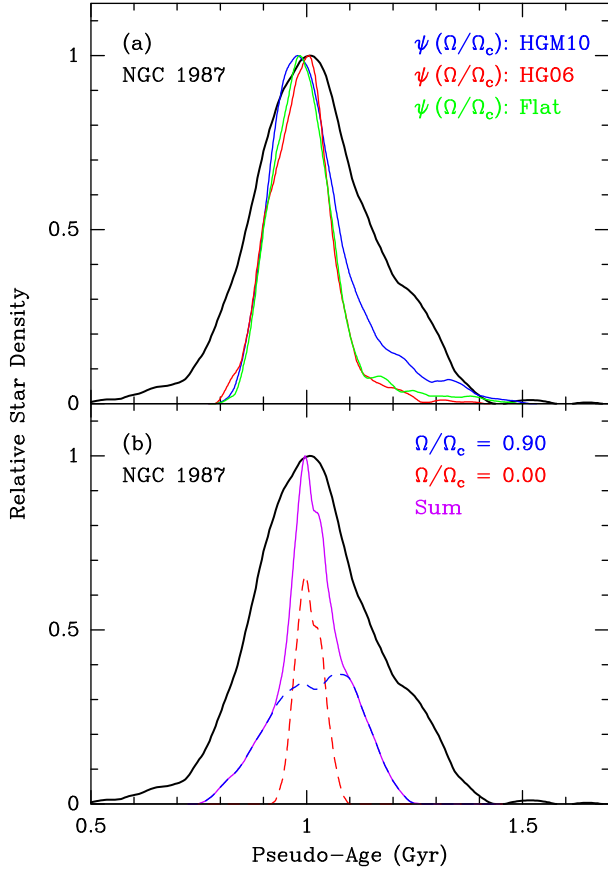


Figure 5. *Panel (a):* The thick black solid line represents the pseudo-age distribution of NGC 1987, while the other solid lines represent the pseudo-age distributions SYCLIST simulations of a cluster with an age of 1.02 Gyr and different distributions of Ω/Ω_c , as indicated in the legend. *Panel (b):* Similar to panel (a), but now the blue and red dashed lines represent the pseudo-age distributions of stars with $\Omega/\Omega_c = 0.9$ and $\Omega/\Omega_c = 0.0$ in the bimodal distribution of D’Antona et al. (2015), respectively. The purple line represents the sum of the two latter distributions. See discussion in Sect. 3.

In the context of the SYCLIST models, one would instead expect the width of eMSTOs to decrease at ages beyond ~ 1.0 Gyr at the metallicities of the LMC and SMC (see also Brandt & Huang 2015), since the MSTO at older ages is populated by stars with $\mathcal{M}/M_\odot < 1.7$ at those metallicities. Such stars have convective envelopes whose angular momentum is decreased considerably by a magnetized wind. Furthermore, the cores of such lower-mass stars are less convective than those with $\mathcal{M}/M_\odot > 1.7$, thus providing less mixing at their core boundaries and allowing less additional “rejuvenating” Hydrogen fuel from the outer regions to burn in their cores⁹. While the current SYCLIST models do not allow one to test this directly, the low pseudo-age spreads found for some of the lower-mass LMC clusters with ages > 1.0 Gyr studied by Correnti et al. (2014) are consistent with the notion that the impact of rotation to the extent of MSTOs indeed diminishes at stellar masses $\mathcal{M}/M_\odot < 1.7$ (see green circles in Figure 2). The increase of the average width of eMSTOs beyond an age of 1.0 Gyr therefore suggests that some property other than stellar rotation is partly responsible for the eMSTO phe-

⁹ Gyr in the study of Piatti & Bastian (2016).

⁹ These complex effects were not accounted for by Brandt & Huang (2015) for stars with $\mathcal{M}/M_\odot < 1.7$. They implicitly assumed that the effects of rotation do not change between 1.45 and 1.7 M_\odot , thus overestimating the effect of rotation on the widths of eMSTOs of Magellanic Cloud clusters at ages $\gtrsim 1.0$ Gyr.

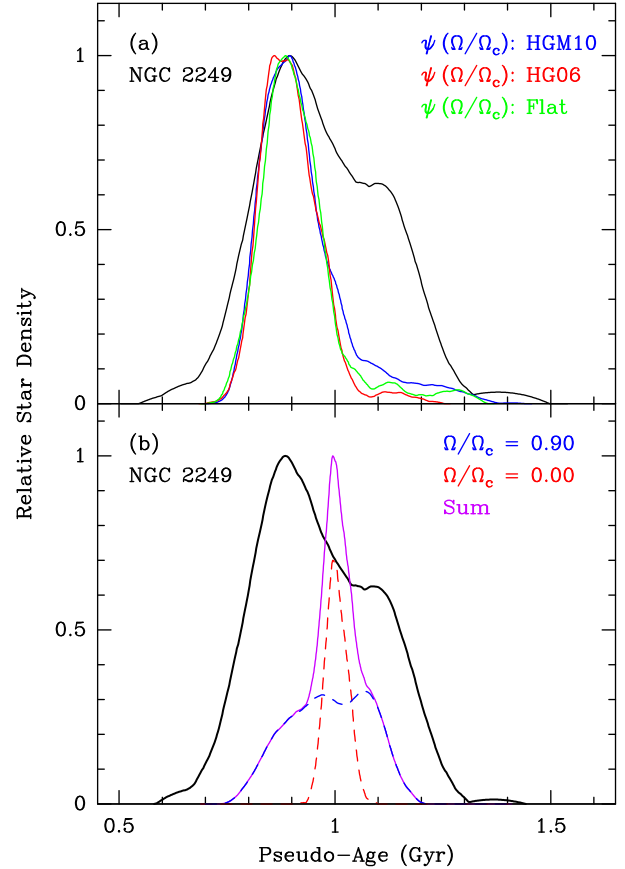


Figure 6. Same as Figure 5, but now for NGC 2249.

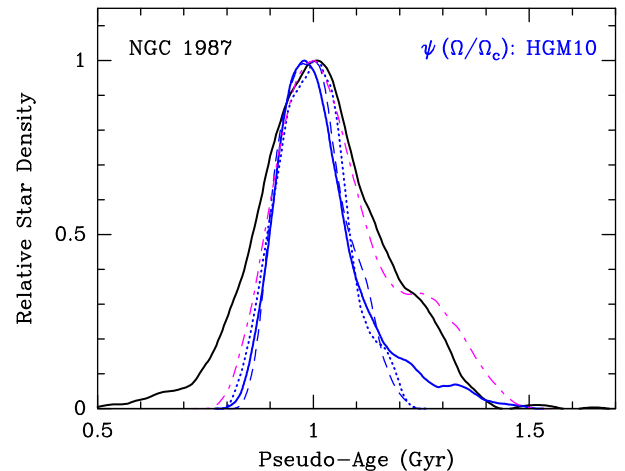


Figure 7. Similar to Figure 5, except that the only SYCLIST simulation shown is the one using the HGM10 distribution of Ω/Ω_c (solid blue line). The dashed and dotted blue lines represent the same SYCLIST simulation, but now ignoring the effects of gravity and limb darkening (dashed blue line) and selecting only stars with viewing angles between 40° and 50° (dotted blue line), respectively, while the magenta dot-dashed line shows the same SYCLIST simulation after selecting only stars with viewing angles between 80° and 90° . See discussion in Sect. 4.1.1.

nomenon, at least for those older clusters.

Another feature among eMSTOs of clusters in the narrow age interval of 1.4–1.7 Gyr is that their widths vary significantly among clusters. This is especially clear in the sample of G+14 (see also Figure 2 and Piatti & Bastian 2016), where the FWHM of the pseudo-age distributions of clusters in this

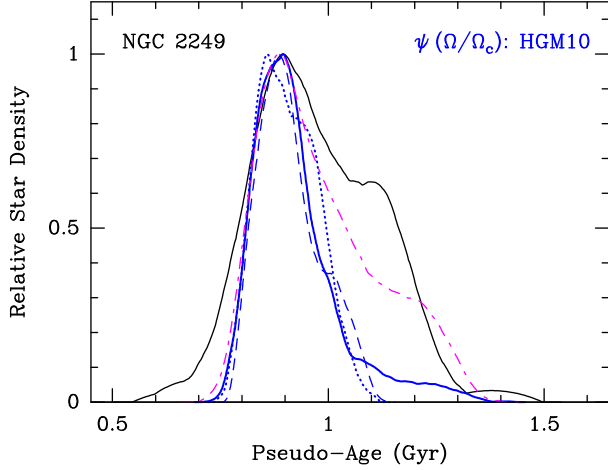


Figure 8. Same as Figure 7, but now for NGC 2249.

age interval ranges between about 200 and 550 Myr and correlates with cluster mass and escape velocity (G+14). Taken at face value, this seems inconsistent with the rotation hypothesis as represented by the current SYCLIST models, since we showed above that the viewing angles already need to be close to equator-on to explain the pseudo-age distributions of NGC 1987 and NGC 2249 (whose FWHMs are only $\lesssim 250$ Myr) in the context of the rotation hypothesis. Conversely, this feature *is* consistent with the “age range” hypothesis of G+14 in which the extent of the eMSTO reflects the period during which the cluster is able to form stars from retained and/or accreted gas at young ages.

4.2. Constraints on Age Spreads

Accepting the evidence for the presence of a wide range of rotation velocities in star clusters from the observations of young massive clusters in the LMC (D’Antona et al. 2015; Milone et al. 2016, 2017; Bastian et al. 2017; Correnti et al. 2017), we now address implications of our results on the “age spread” scenario, i.e., the idea that eMSTOs are mainly due to spreads in stellar age.

Under the assumptions that (i) the distribution of Ω/Ω_C is fairly smooth (rather than showing discrete peaks), especially in the range $0.3 \lesssim \Omega/\Omega_C \lesssim 1.0$, and (ii) the viewing angles of the stellar rotation axes with respect to the line of sight are distributed randomly, the simulations described in the previous sections agree with results of other recent studies in that the presence of a range of stellar rotation rates does increase the extent of MSTOs of simple stellar populations (SSPs). Since our previous investigations of eMSTOs in intermediate-age clusters in the Magellanic Clouds used simulations with non-rotating isochrones to quantify spreads of stellar age necessary to fit pseudo-age distributions (Goudfrooij et al. 2009, 2011a, 2014), one might thus expect that the real age spreads should be smaller. To quantify this for NGC 1987 and NGC 2249, we take the pseudo-age distributions of SYCLIST SSP simulations shown in Figures 5a and 6a and add scaled versions of the same pseudo-age distributions for older stellar ages until we obtain a good fit to the right-hand part of the observed pseudo-age distributions of the cluster in question¹⁰. We use an age step of 0.01 Gyr in this context. Note that this procedure implicitly assumes that

¹⁰ While there is a discrepancy between the observed and simulated pseudo-age distributions of NGC 1987 in the “young” wing as well, we do not put a significant weight on this in view of the uncertainty of the subtrac-

tion of field star contamination in this region of the CMD for this cluster (cf. Figure 3a; Goudfrooij et al. 2011b).

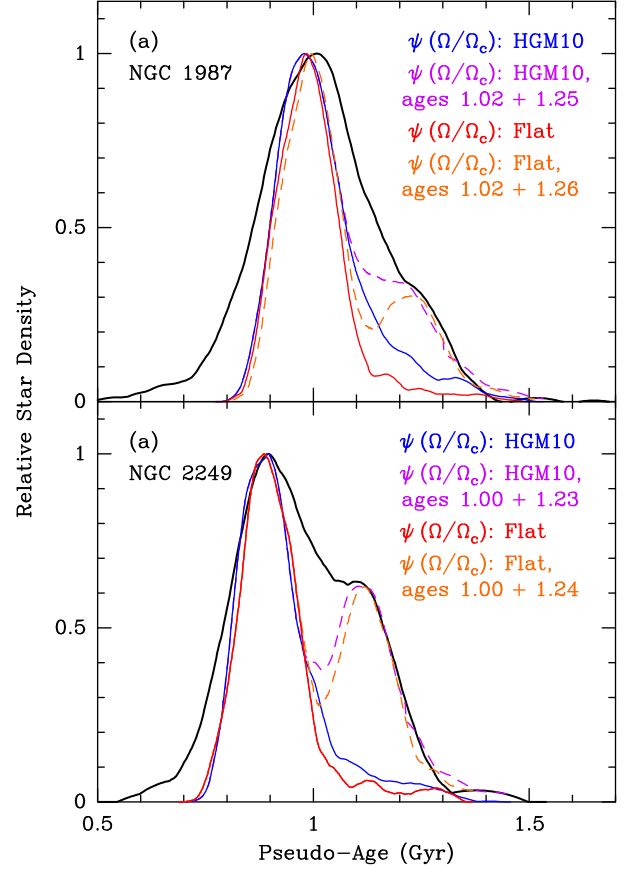


Figure 9. Panel (a): Same as panel (a) of Figure 5, to which we added dashed lines that represent the sum of two SYCLIST cluster simulations involving random viewing angles: the purple line represents the Ω/Ω_C distribution of HGM10 with ages of 1.02 and 1.25 at relative weights of 1.0 and 0.20, respectively, and the orange line represents a flat Ω/Ω_C distribution with ages of 1.02 and 1.26 at relative weights of 1.0 and 0.27, respectively. Panel (b): Same as panel (a) of Figure 6, to which we added dashed lines that represent the sum of two SYCLIST cluster simulations: the purple line represents the Ω/Ω_C distribution of HGM10 with ages of 1.00 and 1.23 at relative weights of 1.0 and 0.53, respectively, and the orange line represents a flat Ω/Ω_C distribution with ages of 1.00 and 1.24 at relative weights of 1.0 and 0.56, respectively. See discussion in Sect. 4.2.

The good fit to the “old” edge of the observed pseudo-age distributions by these simulations illustrates that the inability of the stellar rotation scenario to fit the observed pseudo-age distributions of massive intermediate-age star clusters such as NGC 1987 and NGC 2249 can be effectively overcome by introducing a suitable distribution of stellar ages. In the specific cases of NGC 1987 and NGC 2249, the best-fit age spreads are 235 ± 10 Myr and 235 ± 10 Myr, respectively, where the quoted uncertainties reflect the differences found between the assumptions of the Ω/Ω_C distribution of HGM10 and a flat distribution. These age spreads are similar or somewhat ($\lesssim 15\%$) smaller than those estimated from the FWHM values

tion of field star contamination in this region of the CMD for this cluster (cf. Figure 3a; Goudfrooij et al. 2011b).

of the observed pseudo-age distributions of NGC 1987 and NGC 2249, which were 234 Myr and 262 Myr, respectively (G+14; Correnti et al. 2014). We suggest that the earlier age spread estimates from the overall FWHM values should be regarded as more coarse estimates than the current ones, since the latter account for the effects of wide ranges of stellar rotation rates and also allow for a relative scaling of the numbers of stars at different ages.

Finally, we emphasize that our interpretations mentioned above refer specifically to a comparison of the observed data with predictions of the current SYCLIST models. Given the complex evolutionary and geometric effects of rotation on the spectral energy distribution of stars, it will be important to compare our results with other, future models that incorporate stellar rotation.

5. CONCLUDING REMARKS

In the context of the question of the nature of eMSTOs in young and intermediate-age star clusters in the Magellanic Clouds, we use Monte Carlo simulations with the SYCLIST isochrone models to conduct a detailed investigation of the MSTO morphologies produced by ranges in stellar rotation rates. In doing so, we confirm a recent finding of Niederhofer et al. (2015b) that a distribution of stellar rotation velocities yields an extent of the MSTO that is proportional to the age of the cluster up to an age of ~ 1.0 Gyr, as observed. However, we find that wide ranges of stellar rotation rates yield pseudo-age distributions (derived from cross-cuts across MSTOs in a direction perpendicular to non-rotating isochrones for ages around those of the clusters) that are generally narrower than those observed for clusters at a given age.

We compare the simulations with high-quality CMDs of NGC 1987 and NGC 2249, two massive star clusters in the LMC with an age of ~ 1 Gyr, close to the oldest age for which the MSTO still consists of stars with $\mathcal{M} \geq 1.7 M_{\odot}$, which is the lowest stellar mass modeled in the current SYCLIST models. We find that the distribution of stars across the eMSTOs of these clusters cannot be explained solely by a distribution of stellar rotation velocities, unless the orientations of rapidly rotating stars are heavily biased towards an equator-on configuration. In contrast, a combination of distributions of stellar rotation velocities *and* of stellar ages naturally provides a good fit to the observed eMSTO morphologies. The presence of a wide distribution of stellar rotation velocities diminishes the range in age required to fit the eMSTO morphology of these clusters by $\lesssim 20\%$ relative to results of previous studies that used non-rotating isochrones.

Even though several recent studies have provided important evidence in support of the stellar rotation scenario for the nature of eMSTOs in intermediate-age clusters in the Magellanic Clouds, our results suggest that age spreads of order a few 10^8 yr still seem to be required to fit the detailed morphologies of the eMSTOs in those clusters, especially for the more massive clusters among them (see Sect. 4.1.2). This may seem unexpected, given that a recent study of the very massive cluster W3 ($\mathcal{M} \sim 10^8 M_{\odot}$, age ~ 600 Myr, effective radius $r_{\text{eff}} = 17.5$ pc) in the merger remnant galaxy NGC 7252 did not find any evidence for an extended star formation history (Cabrera-Ziri et al. 2016). We suggest that this paradox might be explained if the ability of clusters to accrete and/or retain gas within its potential well during the first few 10^8 yr after their creation has a significant dependence on its environment, as shown by Conroy & Spergel (2011). Gas present in a cluster formed in a violent dissipative merger of \sim equal-mass

galaxies like NGC 7252 (e.g., Whitmore et al. 1993), involving collisions with relative velocities of hundreds of km s^{-1} , is likely to be stripped rather efficiently (see Conroy & Spergel 2011). In contrast, stripping was likely much less efficient during the relatively quiescent past evolution of dwarf galaxies such as the Magellanic Clouds, thus perhaps allowing the accumulation of accreted or retained gas during the early evolution of massive clusters.

We thank the anonymous referee for thoughtful and useful comments on the manuscript. We are grateful to Sylvia Ekström for promptly answering our questions about the SYCLIST models. Support for this project was provided in part by NASA through grant HST-GO-14174 from the Space Telescope Science Institute, which is operated by the Association of Universities for Research in Astronomy, Inc., under NASA contract NAS5-26555. We acknowledge the use of the R Language for Statistical Computing, see <http://www.R-project.org>.

Facilities: HST(ACS and WFC3)

REFERENCES

- Bastian, N., & de Mink, S. E. 2009, MNRAS, 398, L11
 Bastian, N., Cabrera-Ziri, I., Davies, B., & Larsen, S. S. 2013, MNRAS, 436, 2852
 Bastian, N., Niederhofer, F., Kozhurina-Platais, V., et al. 2016, MNRAS, 460, L20
 Bastian, N., Cabrera-Ziri, I., Niederhofer, F., et al. 2017, MNRAS, 465, 4795
 Bekki, K., & Mackey, A. D. 2009, MNRAS, 394, 124
 Brandt, T. D., & Huang, C. X. 2015, ApJ, 807, 25
 Cabrera-Ziri, I., Bastian, N., Davies, B., et al. 2014, MNRAS, 441, 2754
 Cabrera-Ziri, I., Bastian, N., Hilker, M., et al. 2016, MNRAS, 457, 809
 Carretta, E., Bragaglia, A., Gratton, R. G., et al. 2010, A&A, 505, 117
 Castelli, F., & Kurucz, R. L. 2003, in “Modeling of Stellar Atmospheres”, IAU Symp. No. 210, eds. N. Piskunov et al., Poster A20 (arXiv:astro-ph/0405087)
 Claret, A. 2000, A&A, 363, 1081
 Conroy, C., & Spergel, D. N. 2011, ApJ, 726, 36
 Correnti, M., Goudfrooij, P., Kalirai, J. S., et al. 2014, ApJ, 793, 121
 Correnti, M., Goudfrooij, P., Puzia, T. H., & de Mink, S. E. 2015, MNRAS, 450, 3054
 Correnti, M., Goudfrooij, P., Bellini, A., Kalirai, J. S., & Puzia, T. H. 2017, MNRAS, 467, 3628
 Corsaro, E., Lee, Y.-N., Garcia, R. A., et al. 2017, NatAs, 1, 64
 D’Antona, F., Di Criscienzo, M., Decressin, T., Milone, A. P., Vesperini, E., & Ventura, P. 2015, MNRAS, 453, 2637
 Decressin, T., Meynet, G., Charbonnel, C., Prantzos, N., & Ekström, S. 2007, A&A, 464, 1029
 de Mink, S. E., Pols, O. R., Langer, N., & Izzard, R. G. 2009, A&A, 507, L1
 Ekström, S., Georgy, C., Eggenberger, P., et al. 2012, A&A, 537, A146
 Espinosa Lara, F., & Rieutord, M. 2011, A&A, 533, 43
 For, B.-Q., & Bekki, K. 2017, MNRAS, in press (arXiv:1703.02666)
 Georgy, C., Ekström, S., Granada, A., et al. 2013, A&A, 553, A24
 Georgy, C., Granada, A., Ekström, S., et al. 2014, A&A, 566, A21
 Girardi, L., Rubele, S., & Kerber, L. 2009, MNRAS, 394, L74
 Girardi, L., Eggenberger, P., & Miglio, A. 2011, MNRAS, 412, L103
 Girardi, L., Goudfrooij, P., Kalirai, J. S., et al. 2013, MNRAS, 431, 3501
 Glatt, K., Grebel, E. K., Sabbi, E., et al. 2008, AJ, 135, 1703
 Goudfrooij, P., Puzia, T. H., Kozhurina-Platais, V., & Chandar, R. 2009, AJ, 137, 4988
 Goudfrooij, P., Puzia, T. H., Chandar, R., & Kozhurina-Platais, V. 2011a, ApJ, 737, 4
 Goudfrooij, P., Puzia, T. H., Kozhurina-Platais, V., & Chandar, R. 2011b, ApJ, 737, 3
 Goudfrooij, P., Girardi, L., Kozhurina-Platais, V., et al. 2014, ApJ, 797, 35 (G+14)
 Goudfrooij, P., Girardi, L., Rosenfield, P., et al. 2015, MNRAS, 450, 1693
 Gratton, R., Carretta, E., & Bragaglia, A. 2012, A&A Rev., 20, 50
 Huang, W., & Gies, D. R. 2006, ApJ, 648, 580 (HG06)

- Huang, W., Gies, D. R., & McSwain, M. V. 2010, *ApJ*, 722, 605 (HGM10)
- Keller, S. C., Mackey, A. D., & Da Costa, G. S. 2011, *ApJ*, 731, 22
- Laidler, V. et al. 2008, "Synphot Data User's Guide" (Baltimore: STScI)
- Mackey, A. D., & Broby Nielsen, P. 2007, *MNRAS*, 379, 151
- Mackey, A. D., Broby Nielsen, P., Ferguson, A. M. N., & Richardson, J. C. 2008, *ApJ*, 681, L17
- Milone, A. P., Bedin, L. R., Piotto, G., & Anderson, J. 2009, *A&A*, 497, 755
- Milone, A. P., Bedin, L. R., Cassisi, S., et al. 2013, *A&A*, 555, A143
- Milone, A. P., Bedin, L. R., Piotto, G., et al. 2015, *MNRAS*, 450, 3750
- Milone, A. P., Marino, A. F., D'Antona, F., et al. 2016, *MNRAS*, 458, 4368
- Milone, A. P., Marino, A. F., D'Antona, F., et al. 2017, *MNRAS*, 465, 4363
- Mowlavi, N., Eggenberger, P., Meynet, G., et al. 2012, *A&A*, 541, A41
- Niederhofer, F., Hilker, M., Bastian, N., & Silva-Villa, E. 2015a, *A&A*, 575, 62
- Niederhofer, F., Georgy, C., Bastian, N., & Ekström, S. 2015b, *MNRAS*, 453, 2070
- Piatti, A. E., & Bastian, N. 2016, *MNRAS*, 463, 1632
- Rubele, S., Girardi, L., Kozhurina-Platais, V., Goudfrooij, P., & Kerber, L. 2011, *MNRAS*, 414, 2204
- Rubele, S., Girardi, L., Kozhurina-Platais, V., et al. 2013, *MNRAS*, 433, 2774
- Rubele, S., Kerber, L., & Girardi, L. 2010, *MNRAS*, 403, 1156
- Ventura, P., D'Antona, F., Mazzitelli, I., & Gratton, R. 2001, *ApJ*, 550, L65
- Whitmore, B. C., Schweizer, F., Leitherer, C., Borne, K., & Robert, C. 1993, *AJ*, 106, 1354